Abdelkader ACHAR[1*], Youcef DJERIRI[1], Abderrahim BENTAALLAH[1], Salah HANAFI[1], Mohammed Abdeldjalil DJEHAF[1], Riyadh BOUDDOU[2]

Department of Electrotechnics, Faculty of Electrical Engineering/Intelligent Control and Electrical Power Systems Laboratory, Djillali Liabes University, Sidi Bel-Abbes, Algeria (1)
Department of Technology, Institute of Science and Technology, University Center of Naama, Algeria (2)
ORCID: 1. 0000-0002-9756-5352; 2. 0000-0001-7590-8492; 3. 0000-0001-7982-2346; 4. 0000-0003-3089-7368; 5. 0000-0002-4482-6918; 6. 0000-0001-6555-5785

doi:10.15199/48.2023.04.43

Lyapunov-Based Robust Power Controllers for a Wind Farm Using Parallel Multicell Converters

Abstract. *In this paper, a robust nonlinear control technique for Wind Farm (WF) using a Doubly Fed Induction Generator (DFIG) via a parallel multicell converter (PMC) based on variable speed Wind Energy Conversion Systems (WECS) is presented. The principal concept is to use the backstepping technique to separate the DFIG's active and reactive power rapidly. The Lyapunov function is the foundation for this control strategy, ensuring the system's asymptotic stability. The simulation results show the implemented controller's validity and effectiveness.*

Streszczenie. *W artykule przedstawiono solidną nieliniową technikę sterowania farmą wiatrową (WF) opartą na generatorze indukcyjnym z podwójnym zasilaniem (DFIG) za pośrednictwem równoległego konwertera wieloogniwowego (PMC) stosowanego w systemach konwersji energii wiatrowej o zmiennej prędkości (WECS). Główną koncepcją jest zastosowanie techniki backstepping do solidnego rozdzielenia mocy czynnej i biernej DFIG. Podstawą tej strategii sterowania jest funkcja Lapunowa, która zapewnia asymptotyczną stabilność systemu. Przedstawiono wyniki symulacji, aby wykazać ważność i skuteczność wdrożonego kontrolera. (**Solidne sterowniki mocy oparte na Lapunowie dla farmy wiatrowej z równoległymi konwerterami wielokomórkowymi**)*

Keywords: Wind Farm, DFIG, parallel multicell converter (PMC), backstepping approach, Lyapunov stability.
Słowa kluczowe: Farma wiatrowa, DFIG, równoległy konwerter wieloogniwowy (PMC), podejście wsteczne, stabilność Lapunowa.

I. Introduction

Renewable energy plays a prominent part in meeting total energy needs in the future while preserving the environment and reducing climate change. Global energy consumption has been estimated at an average yearly rate of 2%, the rest by fossil fuels [1]. With known negative effects, many countries have pushed to write challenging strategy goals for renewable energy with reduced greenhouse gas emissions and pollutant emissions, including wind energy. At the expense of the goals outlined in [2], achieving them will lead to a significant rise in the whole quantity of wind energy capacity installed in the next few decades. [3] It gives an overview of predictions for future global expansion of renewable energy sources globally). To achieve that expansion, new, massive wind farms must be planned, built, and upgraded in areas with a high potential for wind energy. Due to its partly rated power electronics converters, variable speed operation, and independent control of power, DFIG-based WF ideas are currently the most popular [4–7]. It has become imperative to improve the control of wind farms to improve energy quality through a robust control technique associated with multilevel converters. In [8] and [9], control coordinates among the wind farm, the power system, and the power load to guarantee a safe and adequate electricity flow. In [8], the backstepping control is proposed, and in [9], the predictive control is suggested. These studies rely on multilevel converters, although no attention was given to power quality in particular. [10] discusses the potential for the coordination, control, and management of various wind farm models to ensure that operational set points for active and reactive power, defined by the Spanish transmission system operator, are met. A hierarchical control structure that extends from the central control level to the control boards of each wind farm and, ultimately, to the level of each wind turbine has been used to develop and implement this coordinated control. This essay will show how both technologies (wind farms with fixed and variable speeds) can help to control the power and voltage. In [11], [12], and [13], an algorithm for power management is presented for the generation of reactive power in every wind turbine generator. The algorithm provides power reference management between the grid side converter (GSC) and the DFIG stator circuit, considering three wind farm operation modes. It also considers the maximum reactive power capability of the DFIG and the GSC. In these studies, the active and reactive power flow from the WECS to the grid is controlled with a vector control based on a conventional PI controller. In [14], [15],[16],[17],[18], and [19], the main idea is to use the backstepping method to robustly separate the active and reactive power of the DFIG in order to maintain system stability. We chose this last control technique from these studies and applied it to the wind farm due to the scarcity of research in this field. In our study, we rely on the excellent energy distribution in the wind farm that is depended on in [11], [12], considering the role of controllers and multilevel converters in improving energy quality and reducing harmonics in the farm. The article is presented as follows: power system configuration is described in section (2). The algorithm based on the proportional distribution of power references is then described in subsection (2. A). The backstepping approach of WF is summarized in detail in subsection (2. B). In subsection (2. C), we discuss modeling the parallel multicell converter (PMC). The simulations in Section 3 show the controller's performance with the wind farm's active and reactive power monitoring and its effectiveness in improving energy quality. Section 4 presents a conclusion.

II. Power system configuration

The grid control forces the operating center to treat the wind farm as a conventional turbine. The study's power system contains four 1.5MW DFIG units connected to the 30kV grid via a 30kV/690V transformer, as shown in figure 1: The WF is based on the DFIG model, as detailed in [16].

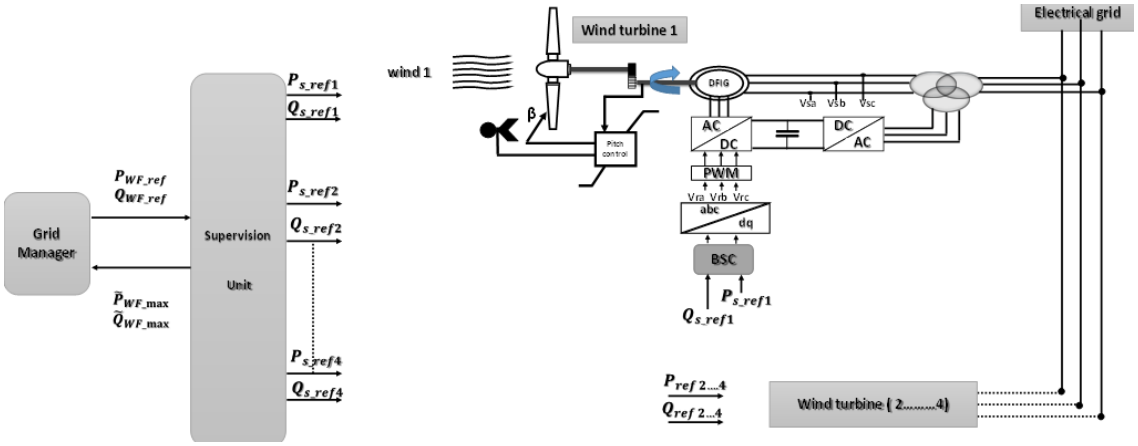

Fig.1. Functional diagram of the studied system

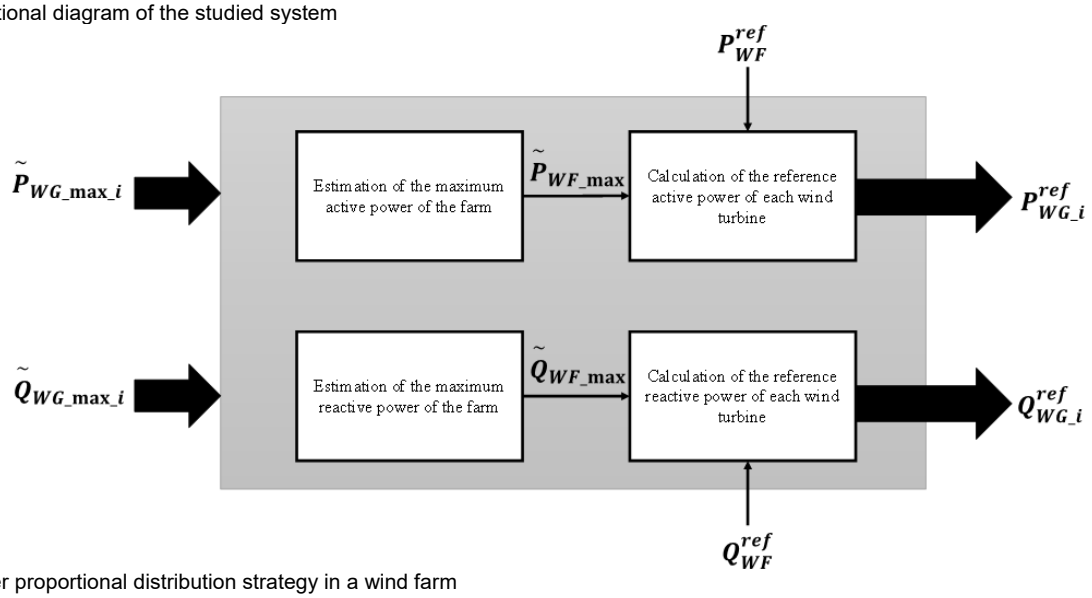

Fig.2. Power proportional distribution strategy in a wind farm

II.1 Proportional power reference distribution-based algorithm

The proportional distribution-based algorithm was created to proportionally distribute the power instructions to the wind turbines on the farm. The advantage of this strategy is that it ensures that all wind farm turbines operate far away from their maximal production capacity. There is, therefore, no risk of turbine saturation. Although one of the turbines is fully loaded, i.e., the turbine is operating at its maximal production or consumption of the

II.2 Backstepping controllers design

Designing the WF backstepping controller can be done in 2 steps [20] :

A. Active Power Control

The active power error is calculated as :

reactant, the missing power is transferred to the other wind turbines that are still capable of satisfying the demand. Nevertheless, implementing this strategy is somewhat complicated as it requires information on the available aerodynamic power of all wind turbines. Moreover, the difficulty of estimating the available aerodynamic power at every wind turbine is directly related to the wind speed (a complex quantity to measure). It, therefore, makes this approach an approximation [11]. The algorithm can be schematized in figure 2.

$$\begin{cases} e_1 = P_{WG\_1}^{ref} - P_{s\_1} \\ \vdots \\ e_n = P_{WG\_n}^{ref} - P_{s\_n} \end{cases} \quad (1)$$

With: n is the DFIG number used on the farm. The derivative of (1) is:

$$\begin{cases} \dot{e}_1 = \dot{P}_{WG\_1}^{ref} - \dot{P}_{s\_1} \\ \vdots \\ \dot{e}_n = \dot{P}_{WG\_n}^{ref} - \dot{P}_{s\_n} \end{cases} \quad (2)$$

Taking V as a Lyapunov candidate function:

$$\begin{cases} V(e_1) = \frac{1}{2} e_1^2 \\ \vdots \\ V(e_n) = \frac{1}{2} e_n^2 \end{cases} \quad (3)$$

The derivative of (3) is given by:

(4)
$$\begin{cases} \dot{V}(e_1) = e_1 \dot{e}_1 = e_1 (\dot{P}^{ref}_{WG\_1} - \dot{P}_{s\_1}) \\ \vdots \\ \dot{V}(e_n) = e_n \dot{e}_n = e_n (\dot{P}^{ref}_{WG\_n} - \dot{P}_{s\_n}) \end{cases}$$

Substituting the power relationship [16] in (4), we get:

(5)
$$\begin{cases} \dot{V}(e_1) = e_1 (\dot{P}^{ref}_{WG\_1} + \frac{3}{2}\frac{L_m}{L_s} \mathrm{V}_s \dot{\mathrm{I}}_{qr\_1}) \\ \vdots \\ \dot{V}(e_n) = e_n (\dot{P}^{ref}_{WG\_n} + \frac{3}{2}\frac{L_m}{L_s} \mathrm{V}_s \dot{\mathrm{I}}_{qr\_n}) \end{cases}$$

Equation (5) becomes, after substituting the derivative:

(6)
$$\begin{cases} \dot{V}(e_1) = e_1 (\dot{P}^{ref}_{WG\_1} + \frac{3}{2}\frac{L_m}{L_s} \mathrm{V}_s (-\mathrm{g}_1 \omega_s \mathrm{I}_{dr\_1} - \\ \frac{R_r}{\sigma L_r} \mathrm{I}_{qr\_1} - \frac{g_1 L_m V_s}{\sigma L_s L_r} + \frac{V_{qr\_1}}{\sigma L_r})) \\ \vdots \\ \dot{V}(e_n) = e_n (\dot{P}^{ref}_{WG\_n} + + \frac{3}{2}\frac{L_m}{L_s} \mathrm{V}_s (-\mathrm{g}_n \omega_s \mathrm{I}_{dr\_n} - \\ \frac{R_r}{\sigma L_r} \mathrm{I}_{qr\_n} - \frac{g_n L_m V_s}{\sigma L_s L_r} + \frac{V_{qr\_n}}{\sigma L_r})) \end{cases}$$

where $\sigma = 1 - (L_m^2 / L_s L_r)$ is the leakage factor, and g is the slippage of the inductor machine. Lastly, the active power stabilizing control law is given by :

(7)
$$\begin{cases} V_{qr\_1} = \frac{2\sigma L_r L_s}{3 L_m V_s} \dot{P}^{ref}_{WG\_1} + \mathrm{g}_1 \omega_s \sigma \mathrm{L}_r \mathrm{I}_{dr\_1} + \\ R_r \mathrm{I}_{qr\_1} - \frac{g_1 L_m V_s}{L_s} - \frac{2\sigma L_r L_s}{3 L_m V_s} K_1 e_1 \\ \vdots \\ V_{qr\_n} = \frac{2\sigma L_r L_s}{3 L_m V_s} \dot{P}^{ref}_{WG\_n} + \mathrm{g}_n \omega_s \sigma \mathrm{L}_r \mathrm{I}_{dr\_n} + \\ R_r \mathrm{I}_{qr\_n} - \frac{g_n L_m V_s}{L_s} - \frac{2\sigma L_r L_s}{3 L_m V_s} K_n e_n \end{cases}$$

In order to guarantee the convergence of the Lyapunov candidate function, we replace the expression (7) in (6) and obtain:

(8)
$$\begin{cases} \dot{V}(\mathrm{e}_1) = -\mathrm{k}_1 e_1^2 < 0 \\ \vdots \\ \dot{V}(\mathrm{e}_n) = -\mathrm{k}_n e_n^2 < 0 \end{cases}$$

Where $k_{1\cdots n}$ is a positive constant.

B. Control of reactive power

The error of reactive power can be given by :

(9)
$$\begin{cases} e_{n+1} = Q^{ref}_{WG\_1} - Q_{s\_1} \\ \vdots \\ e_{2n} = Q^{ref}_{WG\_n} - Q_{s\_n} \end{cases}$$

The derivative of (9) is:

(10)
$$\begin{cases} \dot{e}_{n+1} = \dot{Q}^{ref}_{WG\_1} - \dot{Q}_{s\_1} \\ \vdots \\ \dot{e}_{2n} = \dot{Q}^{ref}_{WG\_n} - \dot{Q}_{s\_n} \end{cases}$$

Considering V as a Lyapunov candidate function:

(11)
$$\begin{cases} V(e_{n+1}) = \frac{1}{2} e_{n+1}^2 \\ \vdots \\ V(e_{2n}) = \frac{1}{2} e_{2n}^2 \end{cases}$$

The derivative of (11) is given by:

(12)
$$\begin{cases} \dot{V}(e_{n+1}) = e_{n+1} \dot{e}_{n+1} = e_{n+1} (\dot{\mathrm{Q}}^{ref}_{WG\_1} - \dot{Q}_{s\_1}) \\ \vdots \\ \dot{V}(e_{2n}) = e_{2n} \dot{e}_{2n} = e_{2n} (\dot{\mathrm{Q}}^{ref}_{WG\_n} - \dot{Q}_{s\_n}) \end{cases}$$

Substituting the power relationship [28] in (12), we get:

(13)
$$\begin{cases} \dot{V}(e_{n+1}) = e_{n+1} (\dot{\mathrm{Q}}^{ref}_{WG\_1} + \frac{3}{2}\frac{L_m}{L_s} \mathrm{V}_s \dot{\mathrm{I}}_{dr\_1}) \\ \vdots \\ \dot{V}(e_{2n}) = e_{2n} (\dot{\mathrm{Q}}^{ref}_{WG\_n} + \frac{3}{2}\frac{L_m}{L_s} \mathrm{V}_s \dot{\mathrm{I}}_{dr\_n}) \end{cases}$$

Equation (13) becomes, after substituting the derivative:

(14)
$$\begin{cases} \dot{V}(e_{n+1}) = e_{n+1} (\dot{\mathrm{Q}}^{ref}_{WG\_1} + \frac{3}{2}\frac{L_m}{L_s} \mathrm{V}_s (\mathrm{g}_1 \omega_s \mathrm{I}_{qr\_1} - \\ \frac{R_r}{\sigma L_r} \mathrm{I}_{dr\_1} + \frac{V_{dr\_1}}{\sigma L_r})) \\ \vdots \\ \dot{V}(e_{2n}) = e_{2n} (\dot{\mathrm{Q}}^{ref}_{WG\_n} + \frac{3}{2}\frac{L_m}{L_s} \mathrm{V}_s (\mathrm{g}_n \omega_s \mathrm{I}_n - \\ \frac{R_r}{\sigma L_r} \mathrm{I}_{dr\_n} + \frac{V_{dr\_n}}{\sigma L_r})) \end{cases}$$

Lastly, the stabilization law of control for active power is defined by :

(15)
$$\begin{cases} V_{dr\_1} = \dfrac{2\sigma L_r L_s}{3L_m V_s}\dot{Q}^{ref}_{WG\_1} - g_1\,\omega_s\sigma L_r I_{qr\_1} + \\ R_r\, I_{dr\_1} - \dfrac{2\sigma L_r L_s}{3L_m V_s} K_{n+1} e_{n+1} \\ \vdots \\ V_{dr\_n} = \dfrac{2\sigma L_r L_s}{3L_m V_s}\dot{Q}^{ref}_{WG\_n} - g_n\,\omega_s\sigma L_r I_{qr\_n} + \\ R_r\, I_{dr\_n} - \dfrac{2\sigma L_r L_s}{3L_m V_s} K_{2n} e_{2n} \end{cases}$$

To ensure the convergence of the Lyapunov candidate function, replacing expression (15) in (14) gives:

(16)
$$\begin{cases} \dot{V}(e_{n+1}) = -k_{n+1}\, e_{n+1}^2 < 0 \\ \vdots \\ \dot{V}(e_{2n}) = -k_{2n}\, e_{2n}^2 < 0 \end{cases}$$

Where $k_{n+1\cdots 2n}$ is a positive constant.

II.3 Modelling of the parallel multicell converter (PMC):

The parallel multicell converter appeared in the early 1990s. This framework comprises an association of switching cells (P) interconnected via independent inductors, also called link inductors. This topology makes it possible to reduce the current constraints on the power electronics switches because each cell is under a constraint equal to I_E / P one since the cells are connected in parallel. Figure 3 shows a parallel multicell converter of P switching cells [21,22].

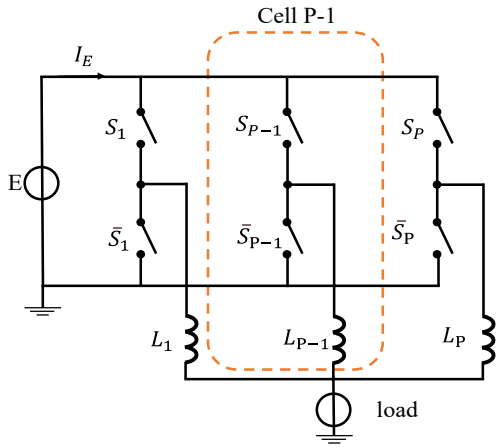

Fig.3. Parallel multicell converter with P switching cells

The work in this paper was done with the parallel multicell converter of 4 (P=4) switching cells and is modelled as follows:

Since we know the value of the inductance, we can obtain the equation governing the evolution of the current:

(17)
$$L_i \frac{d}{dt} I_{L_i} = -R_{L_i} L_{L_i} + V_{L_i}$$

With: i =1 to 4. The voltage V_{Li} is a function of the control signal of the switches S_i.

(18)
$$V_{Li} = S_i \frac{E}{2} - V_s$$

This gives a new expression for the evolution of the current I_{L_i}:

(19)
$$L_i \frac{d}{dt} I_{L_i} + R_{L_i} L_{L_i} = V_{L_i E}$$

The evolution of currents I_{L_i} is governed by equation (19). Thus, the system of equations representing the model at instantaneous values of a parallel multicell arm with four cells operating as an inverter, associated with an R-L load, is:

(20)
$$\begin{cases} \dfrac{d}{dt} I_{L_1} = \dfrac{-R_{L_1} I_{L_1} + S_1 (E/2) - V_s}{L_1} \\ \vdots \\ \dfrac{d}{dt} I_{L_4} = \dfrac{-R_{L_4} I_{L_4} + S_4 (E/2) - V_s}{L_4} \\ \dfrac{d}{dt} V_s = (I_{L_1} + \cdots + I_{L_4}) \dfrac{1}{L_{ch}} - \dfrac{V_s}{L_{ch} R_{ch}} \end{cases}$$

Let us recall the expression of the equation of state with the new matrices:

(21)
$$\dot{X} = A \cdot X + B \cdot S$$

With:

(22)
$$X = \begin{bmatrix} I_{L_1} & I_{L_2} & I_{L_3} & I_{L_4} & V_s \end{bmatrix}^T$$

(23)
$$S = \begin{bmatrix} S_1 & S_2 & S_3 & S_4 \end{bmatrix}^T$$

(24)
$$A = \begin{pmatrix} -\frac{R_{L_1}}{L_1} & 0 & 0 & 0 & -\frac{1}{L_1} \\ 0 & -\frac{R_{L_2}}{L_2} & 0 & 0 & -\frac{1}{L_2} \\ 0 & 0 & -\frac{R_{L_3}}{L_3} & 0 & -\frac{1}{L_3} \\ 0 & 0 & 0 & -\frac{R_{L_4}}{L_4} & -\frac{1}{L_4} \\ \frac{1-S_1}{L_{ch}} & \frac{1-S_2}{L_{ch}} & \frac{1-S_3}{L_{ch}} & \frac{1-S_4}{L_{ch}} & -\frac{1}{L_{ch} R_{ch}} \end{pmatrix}$$

(25)
$$B = \begin{pmatrix} \frac{E_1}{L_1} & 0 & 0 & 0 \\ 0 & \frac{E_1}{L_2} & 0 & 0 \\ 0 & 0 & \frac{E_1}{L_3} & 0 \\ 0 & 0 & 0 & \frac{E_1}{L_4} \\ \frac{I_{L_1}}{I_{ch}} & \frac{I_{L_2}}{I_{ch}} & \frac{I_{L_3}}{I_{ch}} & \frac{I_{L_4}}{I_{ch}} \end{pmatrix}$$

Where: $E_1 = E/2$

III. Simulation results and discussion

The general structure of the proposed wind farm is based on DFIGs powered by parallel multicell converters connected to the power system, as illustrated in Figure 1. This wind farm comprises four generators (DFIG) with the same nominal power of 1.5 MW, the parameters given in the appendix are subjected to four different wind profiles. The backstepping command carries out the control of the multicell converters.

A varied

wind speed operates the WF with a mean value of 8.2 m/s (Figure 4). The MPPT (Maximum Power Point Tracking) strategy generates the active and the reactive power references are maintained as steps. The proportional distribution algorithm ensures the distribution of the reference powers. This production system (wind farm and its central supervision unit) was simulated using MATLAB. Figures 5 (a, b, c, d, e, f, g, h, I, j) show centralized power supervision simulation results in a farm based on a grid operator plan. The farm is operated on an active (Fig.5. a) and reactive (Fig.5. b) power plan imposed by the network manager. This power is distributed in a weighted manner over the three wind turbines (Fig.5.c, d, e, f, g, h, i, j), which shows the application of the proportional distribution algorithm for centralized power supervision in the farm. At t = 2.5s, a third wind turbine disconnection occurred, leading to its production cancellation (Fig.5. g and h). On the other hand, the powers produced by the farm always follow their references (Fig.5. a and b). This is because the other two wind turbines generate more power to fill the power gap.

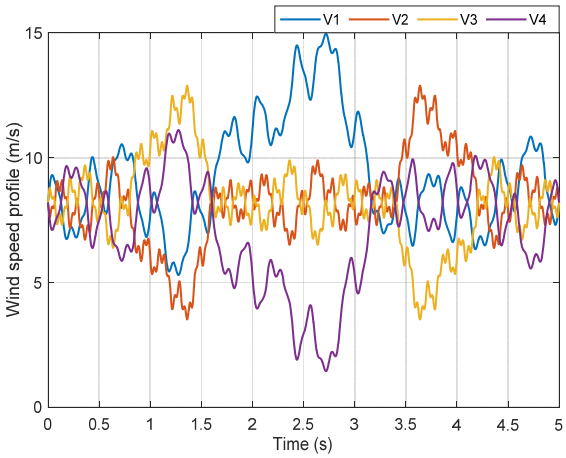

Fig.4. Wind speed profiles for each wind turbine

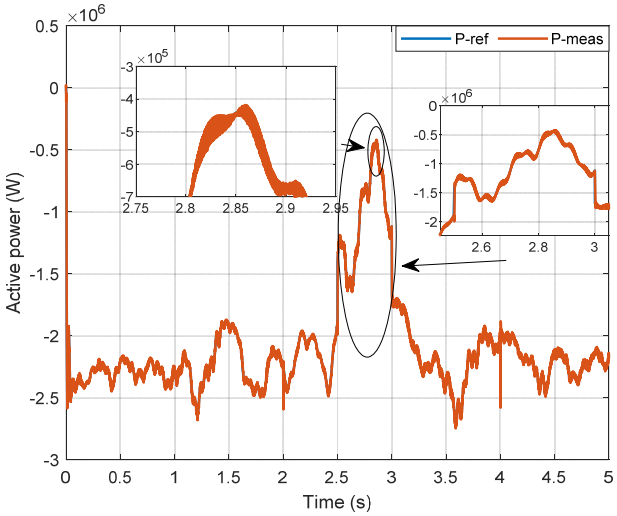

Fig.(5.a). Active power of the farm (reference and simulated)

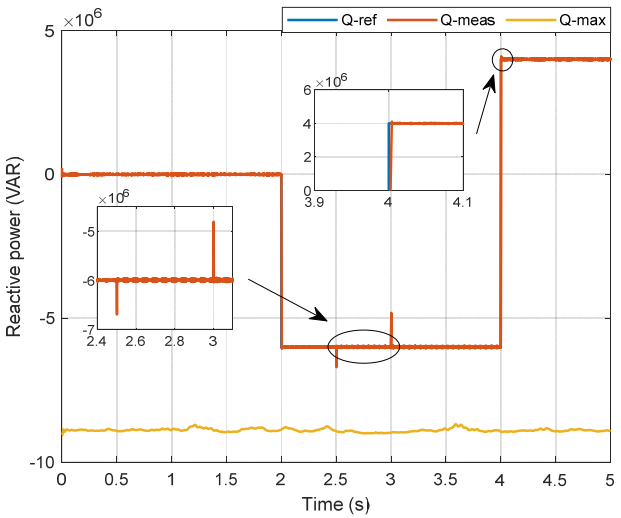

Fig.(5.b). Reactive power of the farm (reference and simulated and maximum)

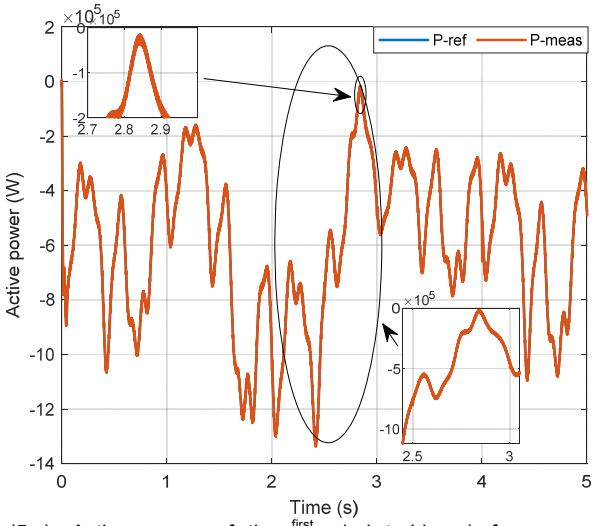

Fig.(5.c). Active power of the first wind turbine (reference and simulated)

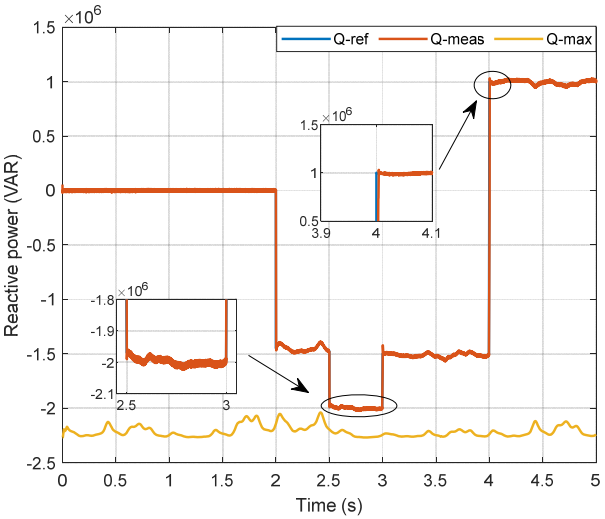

Fig.(5.d). Reactive power of the first wind turbine (reference and simulated and maximum)

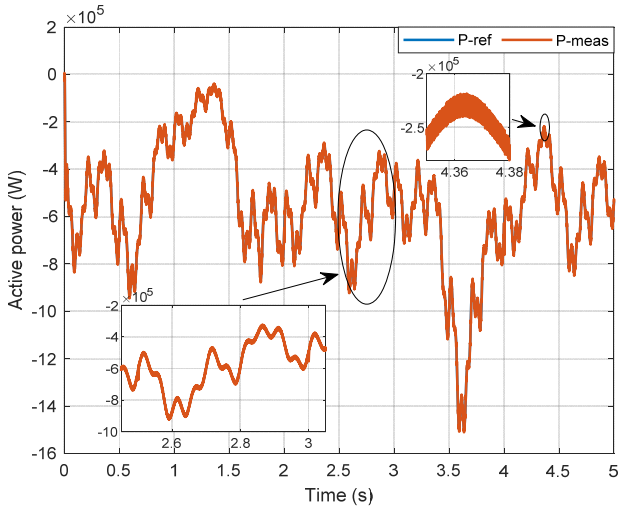

Fig.(5.e). Active power of the second wind turbine (reference and simulated).

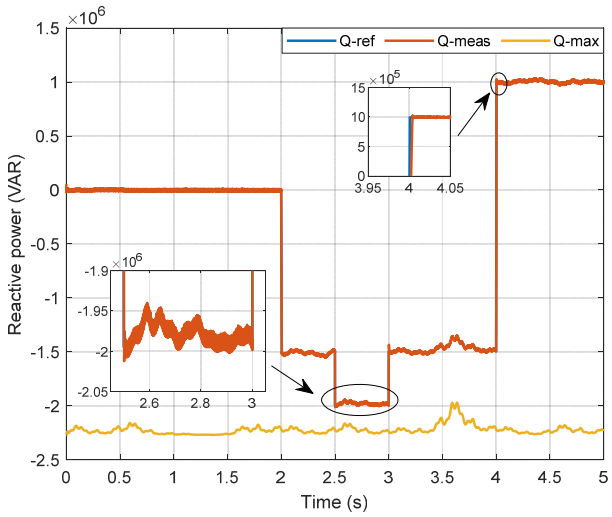

Fig.(5.f). Reactive power of the second wind turbine (reference and simulated and maximum)

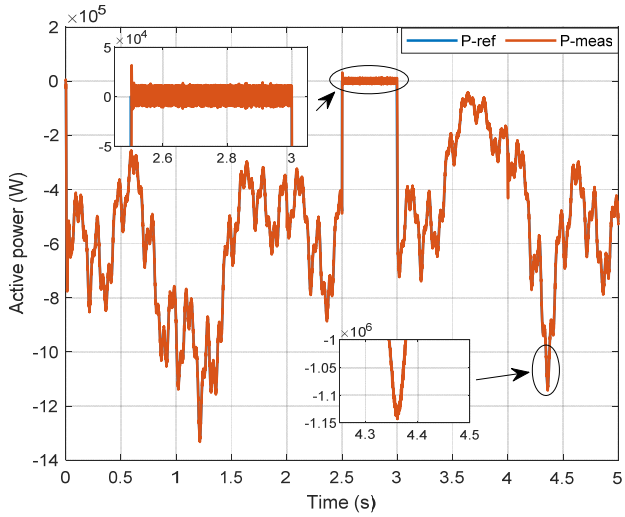

Fig.(5.g). Active power of the third wind turbine (reference and simulated)

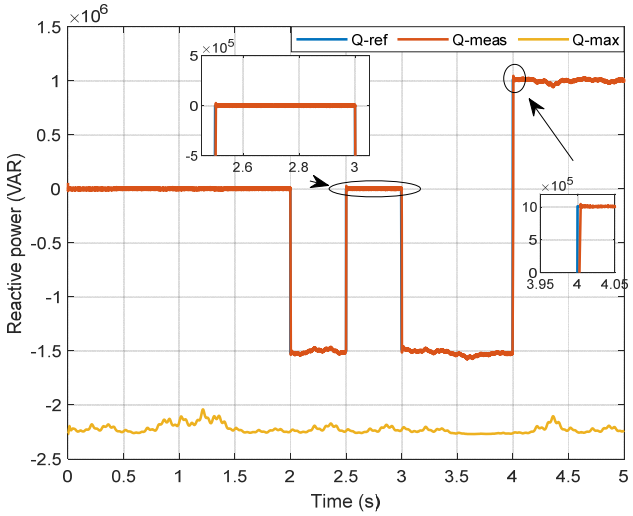

Fig.(5.h). Reactive power of the third wind turbine (reference and simulated and maximum)

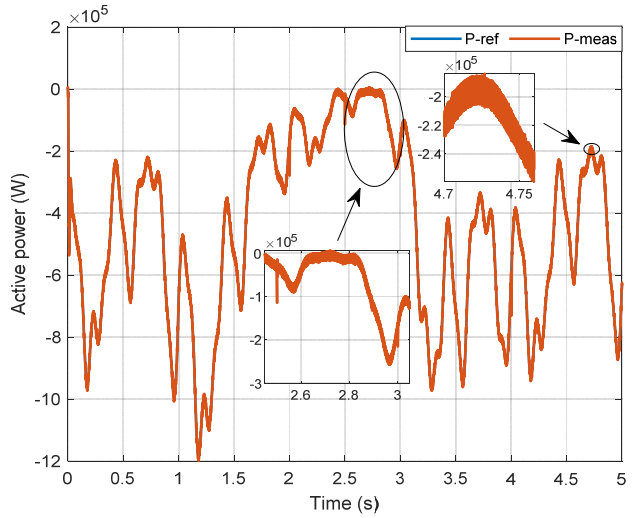

Fig.(5.i). Active power of the fourth wind turbine (reference and simulated

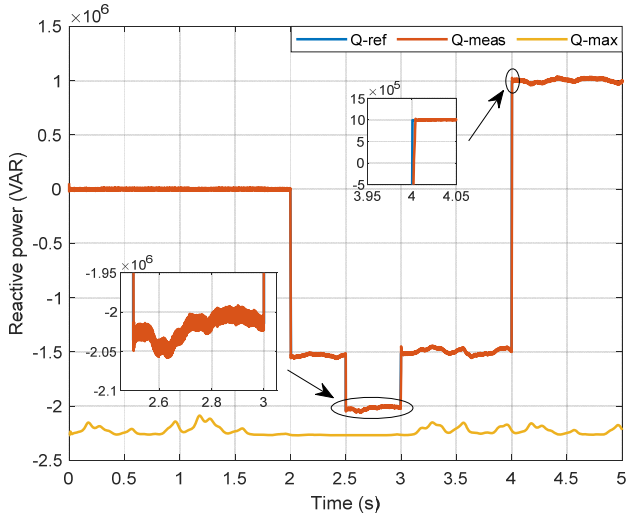

Fig.(5.j). Reactive power of the fourth wind turbine (reference and simulated and maximum)

The THD of the farm electrical current is measured to demonstrate the parallel multicell converter's effectiveness. To do this, a constant speed is imposed on the wind farm and measured by FFT (Fast Fourier Transformation) analysis, as shown in figure 6.

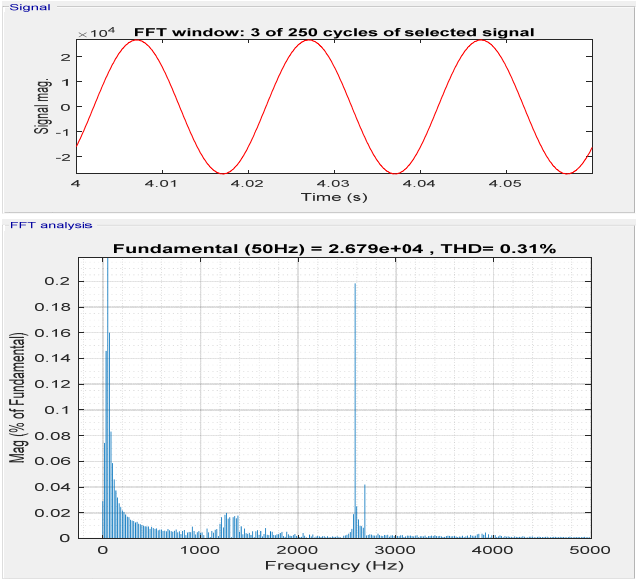

Fig.6. FFT analysis of currents

The proportional distribution algorithm is applied to the central supervision of powers over the operation by deducing the following:

- According to the references imposed by the network operator, perfect control of the active and reactive power, thanks to the backstepping control application.
- All the wind turbines participate, according to the proportional distribution algorithm, in the optimal management of the active and reactive powers of the farm.
- Consideration of the maximum reactive power production capacity of every wind turbine.
- Furthermore, finally, the power quality improved at a low THD thanks to the PMC.

IV. Conclusion

This paper proposes a new topology using parallel multicell converters well adapted to wind farms. Then, a mechanism for managing the active and reactive power of the wind farm connected to the power system is exposed. The centralized supervision of active and reactive powers is based on the proportional distribution algorithm. The proportional distribution algorithm requires estimating the aerodynamic power of every wind turbine; thus, it ensures the operation of the latter without saturation because their power references are defined by taking into account their maximum production capacity. Indeed, it attributes the highest power references to wind turbines with the largest production capacity. Based on specific requests from the grid manager, the central supervision unit distributes the power references for each local supervision unit inside each wind turbine. The supervision algorithm is applied for managing active and reactive power and distributes the references sent by the system operator proportionally. The proportional distribution strategy ensures that each wind turbine works far enough away from its maximum energy production capacity (away from saturation). Backstepping control is offered by integrating all types of active and reactive powers from the farm. With the proposed strategy, the power management was done with excellent performance and with a very high quality of energy transmitted as well as an increase in the total yield of the wind farm.

Appendix

Table 1. presents the parameters of the DFIG used in the study. Table 2 presents the wind turbine parameters.

Table 1. Parameters of DFIG [23]

Rated power, P_n	1.5 MW
Nominal wind speed, v	12.5 m/s
Stator rated voltage, V_s	398/690 V
Stator Rated current, I_n	1900 A
Stator rated frequency, f	50 Hz
Stator inductance, L_s	0.0137 H
Rotor inductance, L_r	0.0136 H
Mutual inductance, M	0.0135 H
Stator resistance, R_s	0.012 Ω
Rotor resistance, R_r	0.021 Ω
Number of pairs of poles, p	2
Total inertia J	1000kg.m2

Table 2. Wind turbine parameters [23]

Number of blades	3
The radius of the rotor R	35.25 m
Speed multiplier gain G	90
Total moment of inertia J	1000 Kg.m2
Viscous friction coefficient f_v	0.0024N.m.s-1
Starting wind speed V_d	4m/s
Stopping wind speed V_m	25m/s

Authors

Mr. Abdelkader ACHAR. Department of Electrotechnics, Faculty of Electrical Engineering/Intelligent Control and Electrical Power Systems Laboratory, Djillali Liabes University, Sidi Bel-Abbes, Algeria, E-mail: abdelkader.achar@univ-sba.dz.

Dr. Youcef DJERIRI. Department of Electrotechnics, Faculty of Electrical Engineering/Intelligent Control and Electrical Power Systems Laboratory, Djillali Liabes University, Sidi Bel-Abbes, Algeria, E-mail: youcef.djeriri@univ-sba.dz.

Prof. Abderrahim BENTAALLAH. Department of Electrotechnics, Faculty of Electrical Engineering/Intelligent Control and Electrical Power Systems Laboratory, Djillali Liabes University, Sidi Bel-Abbes, Algeria, E-mail: abderrahim.bentaallah@univ-sba.dz

Dr. Salah HANAFI. Department of Electrotechnics, Faculty of Electrical Engineering/Intelligent Control and Electrical Power Systems Laboratory, Djillali Liabes University, Sidi Bel-Abbes, Algeria, E-mail: salah.hanafi@univ-sab.dz

Dr. Mohammed Abdeldjalil DJEHAF. Department of Electrotechnics, Faculty of Electrical Engineering/Intelligent Control and Electrical Power Systems Laboratory, Djillali Liabes University, Sidi Bel-Abbes, Algeria, E-mail: med_djehaf@yahoo.com

Dr. Riyadh BOUDDOU. Department of Electrotechnics, Faculty of Electrical Engineering/IRECOM Laboratory, Djillali Liabes University, Sidi Bel-Abbes, Algeria, Department of Technology, Institute of Science and Technology, University Center of Naama, IEEE Member, Algeria. E-mail: riyadh.bouddou@ieee.org

REFERENCES

[1] IEA (2018) Global energy and CO2 status report. *International Energy*, Technical report. *Agency*. 2017. https://www.iea.org/publications/freepublications/publication/GECO2017.pdf

[2] REN21 (2018) Renewables—global status report, renew energy policy network for the 21st century (REN21). Technical report. REN21 Secretariat, Paris. 2018. http://www.ren21.net/status-of-renewables/globalstatus-report/

[3] REN21 (2017) *Renewables global futures report (GFR).* Technical report, renew energy policy network for the 21st century (REN21). REN21 Secretariat, Paris. 2017. http://www.ren21.net/future-of-renewables/globalfutures-report/

[4] PENA, Ruben, CLARE, J. C., et ASHER, G. M. Doubly fed induction generator using back-to-back PWM converters and its application to variable-speed wind-energy generation. *IEE Proceedings-Electric power applications*, 143 (1996), No. 3, 231-241.

[5] MULLER, Set, DEICKE, M., et DE DONCKER, Rik W. Doubly fed induction generator systems for wind turbines. *IEEE Industry applications magazine*, 8 (2002), No. 3, 26-33.

[6] Akel, F., Ghennam, T., Berkouk, E. M., & Laour, M. (2014). An improved sensorless decoupled power control scheme of grid connected variable speed wind turbine generator. *Energy Conversion and Management*, 78 (2014), 584-594.
[7] Lopez, J., Sanchis, P., Roboam, X., & Marroyo, L. Dynamic behaviour of the doubly fed induction generator during three-phase voltage dips. *IEEE Transactions on Energy conversion*, 22(2007), No. 3, 709-717.
[8] Belabbas, B., Denai, M., & Allaoui, T. Hierarchical energy management and control to improve the reliability and efficiency of wind farms connected to the grid. *International Transactions on Electrical Energy Systems*, 30(2020), No. 7, e12400.
[9] Chikha, S., Barra, K., & Reama, A. Predictive current control of a wind energy conversion system based DFIG via direct matrix converter. *In IREC2015 The Sixth International Renewable Energy Congress* (pp. 1-7). 2015, March, IEEE.
[10] Rodriguez-Amenedo, J. L., Arnaltes, S., & Rodriguez, M. A. Operation and coordinated control of fixed and variable speed wind farms. *Renewable energy*, 33(2008), No. 3, 406-414.
[11] Ghennam, T., Aliouane, K., Akel, F., Francois, B., & Berkouk, E. M. Advanced control system of DFIG based wind generators for reactive power production and integration in a wind farm dispatching. *Energy Conversion and Management*, 105 (2015), 240-250.
[12] Atallah, M., Mezouar, A., Belgacem, K., Benmahdjoub, M. A., Saidi, Y., & Brahmi, B. Power Control and Management of DFIGs Wind Farm Equipped with Aggregation Methods by Using Local Supervision Unit Based on S-Function Builder. *Journal of Control, Automation and Electrical Systems*, 33(2022), No. 3, 912-928.
[13] Ouled Amor, W., Ghariani, M., & Guesmi, S. The electric production distribution method supervises a wind farm connected to the grid. *International Journal Of Renewable Energy Research*, 5(2015), No. 4, 944-951.
[14] Bouchiba, N., Barkia, A., Sallem, S., Chrifi-Alaoui, L., Drid, S., & Kammoun, M. B. A. Implementation and comparative study of control strategies for an isolated DFIG based WECS. *The European Physical Journal Plus*, 132(2017), No. 10, 1-13.
[15] Dbaghi, Y., Farhat, S., Mediouni, M., Essakhi, H., & Elmoudden, A. Indirect power control of DFIG based on wind turbine operating in MPPT using backstepping approach. *International Journal of Electrical and Computer Engineering*, 11(2021), No. 3, 1951.
[16] Djeriri, Y. Lyapunov-based robust power controllers for a doubly fed induction generator. *Iranian Journal of Electrical and Electronic Engineering*, 16(2020), No. 4, 551-558.
[17] Mechter, A., Kemih, K., & Ghanes, M. Backstepping control of a wind turbine for low wind speeds. *Nonlinear Dynamics*, 84(2016), No. 4, 2435-2445.
[18] Hamid, C., Derouich, A., Hallabi, T., Zamzoum, O., Taoussi, M., Rhaili, S., & Boulkhrachef, O. Performance improvement of the variable speed wind turbine driving a DFIG using nonlinear control strategies. *International Journal of Power Electronics and Drive Systems*, 12(2021), No.4, 2470.
[19] Yessef, M., Bossoufi, B., Taoussi, M., Lagrioui, A., & El Mahfoud, M. Evaluation of adaptive backstepping control applied to DFIG wind system used on the real wind profile of the Dakhla-Morocco City. *In WITS* (pp. 661-671). Springer, 2022. Singapore.
[20] Dbaghi, Y., Farhat, S., Mediouni, M., Essakhi, H., & Elmoudden, A. Indirect power control of DFIG based on wind turbine operating in MPPT using backstepping approach. *International Journal of Electrical and Computer Engineering*, 11(2021), No. 3, 1951.
[21] Hanafi, S., Fellah, M. K., Yaichi, M., & Benkhoris, M. F. Control of stacked multicellular inverter. *Cell*, 12, (2016), C11.
[22] Hanafi, S., Fellah, M. K., Guebli, A., & Chiali, E. Control with cyclic reports modulation of 3x2 stacked multicellular DC/AC converter. *Cell*, 11 (2014), 21.
[23] DJERIRI, Y. Robust second order sliding mode control of doubly-fed induction generator for wind energy conversion system. *Acta Electrotechnica et Informatica*, 20(2020), No. 3, 30-38.